应用数学和力学，第11卷第10期（1990年10月）
Applied Mathematics and Mechanics

应用数学和力学编委会编
重庆出版社出版

矩形板屈曲和后屈曲弹塑性分析*

沈惠申

（上海交通大学，1989年3月29日收到）

摘　要

本文以摄动法给出了矩形板屈曲和后屈曲全过程的弹塑性分析.

本文同时讨论了初始几何缺陷对矩形板后屈曲性态的影响．计算结果表明，矩形板非弹性屈曲对初始缺陷是敏感的．计算结果与实验结果的比较表明二者相当一致.

关键词　结构稳定性，非弹性屈曲，后屈曲，矩形板

一、引　言

压缩简支矩形板在非弹性范围内的屈曲和后屈曲性态是一个相当复杂而又尚未搞清的问题.

众所周知，经典的塑性屈曲分析导致一个明显的矛盾，即按塑性形变理论计算所得的屈曲载荷要比按塑性流动理论计算所得的结果更接近实验数据.

存在于流动理论和实验结果之间的差异常被解释为是由于板的初始几何缺陷所造成的[1,2]．事实上，板的弹性屈曲对初始几何缺陷是不敏感的[3,4]．然而，当板的屈曲发生在塑性范围时情况将有很大的不同．Ractliffe (1968)[5] 的实验研究业已表明，当非弹性应变超过屈服点后，板的承载能力会出现突然的、明显的下降，其后屈曲性态有类似轴压圆柱薄壳弹性屈曲的表现．此种情况对于工程结构来讲是危险的．70年代初期某些板梁桥结构的破坏证实了这一点，并对板结构设计者们提出一个警告，说明对板的工作表现在很多方面还需要加以研究.

70年代以来，国外许多学者对板的非弹性屈曲和后屈曲全过程作过诸多数值分析[6~11]．大多数作者采用能量法、有限元法或有限差分法，因此，这些分析完全依赖于大型、高速计算机．即使如此，由于大挠度带来的几何非线性和由于屈服所造成的物理非线性，使得问题的分析变得非常困难．至今尚未得到满意的结果.

Korol和Sherbourne(1972)[12]，以及Davies 等(1975)[13]完全从另一种角度来处理这一问题，他们讨论了压缩简支矩形板的破坏机理，指出可用加载曲性和卸载曲线的交点来表征板的极值载荷．其不足是仅考虑了刚-塑性模型，并且无法计及板初始几何缺陷的影响．对

* 卢文达推荐.

于屈曲载荷超过屈服点的板此种分析还不足以给出满意的解释。

在文[3,4]中，作者曾以挠度为摄动参数，采用摄动法研究了各向同性和正交各向异性矩形板在面内压缩作用下的弹性屈曲和后屈曲，取得了满意的结果。这一方法将在本文中得到进一步的推广运用，给出四边简支矩形板屈曲和后屈曲全过程的弹塑性分析。

本文同时讨论初始几何缺陷对板屈曲和后屈曲性态的影响。初始几何缺陷的形式取作和矩形板小挠度解的形式一致。

二、分析方法与渐近解

假定四边简支矩形板的长为 a，宽为 b，厚度为 t，受到对边均布压力。取坐标系如图1所示。以 W^* 和 W 分别表示初始的和附加的挠度。以 ϕ 表示应力函数。引进

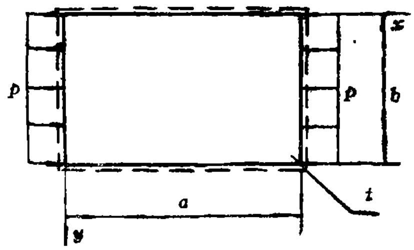

图 1 单向压缩简支矩形板

$$x=\frac{\pi}{a}X,\quad y=\frac{\pi}{b}Y,\quad \beta=\frac{a}{b},\quad w=\frac{W}{\sqrt[4]{a_{11}a_{22}d_{11}d_{22}}}$$

$$w^*=\frac{W^*}{\sqrt[4]{a_{11}a_{22}d_{11}d_{22}}},\quad \varphi=\frac{\phi}{\sqrt{d_{11}d_{22}}}$$

$$\gamma_1=\frac{d_{12}+2d_{66}}{d_{11}},\quad \gamma_2^2=\frac{d_{22}}{d_{11}}=\frac{a_{11}}{a_{22}},\quad \gamma_3=\frac{a_{12}+a_{66}/2}{a_{22}}$$

$$\nu_e=-\frac{a_{12}}{a_{22}},\quad \lambda_x=\frac{\sigma_x b^2 t}{4\pi^2\sqrt{d_{11}d_{22}}},\quad \delta_x=\frac{b^2}{4\pi^2\sqrt{a_{11}a_{22}d_{11}d_{22}}}\frac{\varDelta_x}{a}$$

那么，板的大挠度方程可表为如下无量纲形式

$$L_1w=\gamma_2\beta^2\left[\frac{\partial^2\varphi}{\partial y^2}\frac{\partial^2 w}{\partial x^2}-2\frac{\partial^2\varphi}{\partial x\partial y}\frac{\partial^2 w}{\partial x\partial y}+\frac{\partial^2\varphi}{\partial x^2}\frac{\partial^2 w}{\partial y^2}+\frac{\partial^2\varphi}{\partial y^2}\frac{\partial^2 w^*}{\partial x^2}-2\frac{\partial^2\varphi}{\partial x\partial y}\frac{\partial^2 w^*}{\partial x\partial y}+\frac{\partial^2\varphi}{\partial x^2}\frac{\partial^2 w^*}{\partial y^2}\right] \tag{2.1}$$

$$L_2\varphi=\gamma_2\beta^2\left[\left(\frac{\partial^2 w}{\partial x\partial y}\right)^2-\frac{\partial^2 w}{\partial x^2}\frac{\partial^2 w}{\partial y^2}+2\frac{\partial^2 w}{\partial x\partial y}\frac{\partial^2 w^*}{\partial x\partial y}-\frac{\partial^2 w}{\partial x^2}\frac{\partial^2 w^*}{\partial y^2}-\frac{\partial^2 w}{\partial y^2}\frac{\partial^2 w^*}{\partial x^2}\right] \tag{2.2}$$

其中

$$\left.\begin{aligned} L_1&=\frac{\partial^4}{\partial x^4}+2\gamma_1\beta^2\frac{\partial^4}{\partial x^2\partial y^2}+\gamma_2^2\beta^4\frac{\partial^4}{\partial y^4}\\ L_2&=\frac{\partial^4}{\partial x^4}+2\gamma_3\beta^2\frac{\partial^4}{\partial x^2\partial y^2}+\gamma_2^2\beta^4\frac{\partial^4}{\partial y^4}\end{aligned}\right\}\tag{2.3}$$

边界支承假定为四边简支的，那么边界条件为

$$x=0,\ \pi;\quad w=w_{,xx}=0,\ \varphi_{,xy}=0\tag{2.4a}$$

$$\frac{1}{\pi}\int_0^\pi\beta^2\frac{\partial^2\varphi}{\partial y^2}dy+4\lambda_x\beta^2=0\tag{2.4b}$$

$$y=0,\ \pi;\quad w=w_{,yy}=0,\ \varphi_{,xy}=0\tag{2.5a}$$

$$\frac{1}{\pi}\int_0^\pi\frac{\partial^2\varphi}{\partial x^2}dx=0\tag{2.5b}$$

板的单位轴向缩短为

$$\delta_x=-\frac{1}{4\pi^2\beta^2\gamma_2}\int_0^\pi\int_0^\pi\left[\left(\gamma_2^2\beta^2\frac{\partial^2\varphi}{\partial y^2}-\nu_e\frac{\partial^2\varphi}{\partial x^2}\right)-\frac{1}{2}\gamma_2\left(\frac{\partial w}{\partial x}\right)^2-\gamma_2\frac{\partial w}{\partial x}\frac{\partial w^*}{\partial x}\right]dxdy\tag{2.6}$$

对于板的屈曲和后屈曲全过程分析需要同时考虑加载曲线和卸载曲线。

2.1 加载曲线

（1） 当$\sigma_x<\sigma_0$(板的屈服应力)时，采用弹性板方程，即Kármán板方程，此时[3]

$$\left.\begin{aligned} &\gamma_1=\gamma_2=\gamma_3=1,\quad w=\frac{W}{t}\sqrt{12(1-\nu^2)}\\ &w^*=\frac{W^*}{t}\sqrt{12(1-\nu^2)},\quad \varphi=\frac{\phi}{D}\\ &\lambda_x=\frac{\sigma_x b^2 t}{4\pi^2 D},\quad \delta_x=\frac{12(1-\nu^2)(b/t)^2}{4\pi^2}\frac{\Delta_x}{a}\end{aligned}\right\}\tag{2.7}$$

其中D为弯曲刚度，E和ν分别为弹性模数和Poisson比。

（2） 当$\sigma_0\leqslant\sigma_x$时，采用塑性板方程[14]。板的非弹性分析需要给出材料的应变强化曲线（或应力-应变关系）。

按塑性流动理论，此时

$$\left.\begin{aligned} \gamma_1&=\frac{(1+\nu)(1+E_t/E)+(5-4\nu)(1-E_t/E)/2}{2(1+\nu)(1/4+(3/4)(E_t/E))}\\ \gamma_2^2&=\frac{1}{1/4+(3/4)(E_t/E)},\quad \gamma_3=\frac{(3/2)(E_t/E)-1/2}{1/4+(3/4)(E_t/E)}\\ w&=\frac{W}{t}\gamma_2\sqrt{3\frac{E_t}{E}\left[(5-4\nu)-(1-2\nu)^2\frac{E_t}{E}\right]}\\ w^*&=\frac{W^*}{t}\gamma_2\sqrt{3\frac{E_t}{E}\left[(5-4\nu)-(1-2\nu)^2\frac{E_t}{E}\right]}\end{aligned}\right\}\tag{2.8}$$

$$\left.\begin{aligned}
\varphi &= 3\left[(5-4\nu)-(1-2\nu)^2\frac{E_t}{E}\right]\frac{\phi\gamma_2}{Et^3}\\
\lambda_s &= 3\left[(5-4\nu)-(1-2\nu)^2\frac{E_t}{E}\right]\frac{\sigma_s(b/t)^2\gamma_2}{4\pi^2 E}\\
\delta_s &= \frac{3(E_t/E)[(5-4\nu)-(1-2\nu)^2(E_t/E)]\gamma_2^2(b/t)^2}{4\pi^2}\frac{\Delta_s}{a}
\end{aligned}\right\}$$

按塑性形变理论，此时

$$\left.\begin{aligned}
\gamma_1 &= \frac{3+(1/2)(1-2\nu)(E_s/E)-(3/2)(1-2\nu)E_t/E}{[3-(1-2\nu)(E_s/E)](1/4+(3/4)(E_t/E_s))}\\
\gamma_2^2 &= \frac{1}{1/4+(3/4)(E_t/E_s)},\quad \gamma_3=\frac{(3/2)(E_t/E_s)-1/2}{1/4+(3/4)(E_t/E_s)}\\
w &= \frac{W}{t}\gamma_2\sqrt{3\frac{E_t}{E_s}\left[3+2(1-2\nu)\frac{E_s}{E}-(1-2\nu)^2\frac{E_t}{E}\frac{E_s}{E}\right]}\\
w^* &= \frac{W^*}{t}\gamma_2\sqrt{3\frac{E_t}{E_s}\left[3+2(1-2\nu)\frac{E_s}{E}-(1-2\nu)^2\frac{E_t}{E}\frac{E_s}{E}\right]}\\
\varphi &= 3\left[3+2(1-2\nu)\frac{E_s}{E}-(1-2\nu)^2\frac{E_t}{E}\frac{E_s}{E}\right]\frac{\phi\gamma_2}{E_s t^3}\\
\lambda_s &= 3\left[3+2(1-2\nu)\frac{E_s}{E}-(1-2\nu)^2\frac{E_t}{E}\frac{E_s}{E}\right]\frac{\sigma_s(b/t)^2\gamma_2}{4\pi^2 E_s}\\
\delta_s &= \frac{3(E_t/E_s)[3+2(1-2\nu)(E_s/E)-(1-2\nu)^2(E_t/E)(E_s/E)]\gamma_2^2(b/t)^2}{4\pi^2}\\
&\quad\cdot\frac{\Delta_s}{a}
\end{aligned}\right\}\tag{2.9}$$

其中E_t，E_s分别为单向拉伸曲线的切线模数和割线模数。

对于(1)和(2)两种加载过程，取方程(2.1)和(2.2)的解为如下渐近展开式

$$w(x,y,\varepsilon)=\sum_{k=1}\varepsilon^k w_k(x,y),\quad \varphi(x,y,\varepsilon)=\sum_{k=0}\varepsilon^k\varphi_k(x,y)\tag{2.10}$$

并假定无量纲初挠度为

$$w^*(x,y,\varepsilon)=\varepsilon A_{11}^*\sin mx\sin ny=\varepsilon\mu_1 A_{11}^{(1)}\sin mx\sin ny\tag{2.11}$$

将式(2.10)、(2.11)代入方程(2.1)、(2.2)，便可获得各级摄动方程，逐级摄动，我们可以得到大挠度渐近解

$$\begin{aligned}
w=\ &\varepsilon[A_{11}^{(1)}\sin mx\sin ny]+\varepsilon^3[A_{13}^{(3)}\sin mx\sin 3ny\\
&+A_{31}^{(3)}\sin 3mx\sin ny]+O(\varepsilon^5)
\end{aligned}\tag{2.12}$$

$$\begin{aligned}
\varphi=&-B_{00}^{(0)}\frac{y^2}{2}+\varepsilon^2\left[-B_{00}^{(2)}\frac{y^2}{2}+B_{20}^{(2)}\cos 2mx+B_{02}^{(2)}\cos 2ny\right]\\
&+\varepsilon^4\left[-B_{00}^{(4)}\frac{y^2}{2}+B_{20}^{(4)}\cos 2mx+B_{02}^{(4)}\cos 2ny\right.\\
&+B_{22}^{(4)}\cos 2mx\cos 2ny+B_{40}^{(4)}\cos 4mx+B_{04}^{(4)}\cos 4ny
\end{aligned}$$

$$+B_{24}^{(4)}\cos 2mx\cos 4ny+B_{42}^{(4)}\cos 4mx\cos 2ny\Big]+O(\varepsilon^6) \tag{2.13}$$

按文[4]，我们可以进一步导得以最大无量纲挠度为摄动参数的表达式

$$\lambda_s=\frac{1}{4\beta^2\gamma_2}\Big\{\frac{m^4+2\gamma_1 m^2n^2\beta^2+\gamma_2^2n^4\beta^4}{(1+\mu_1)m^2}+\frac{1}{16}\frac{m^4+\gamma_2^2n^4\beta^4}{m^2}(1+2\mu_1)w_m^2+\frac{1}{256m^2}$$
$$\cdot\Big\langle 2(1+\mu_1)^2(1+2\mu_1)^2\Big[\frac{m^4(m^4+\gamma_2^2n^4\beta^4)}{g_{13}}+\frac{\gamma_2^2n^4\beta^4(m^4+\gamma_2^2n^4\beta^4)}{g_{31}}\Big]$$
$$-(1+\mu_1)(1+2\mu_1)[2(1+\mu_1)^2+(1+2\mu_1)]$$
$$\cdot\Big[\frac{m^8}{g_{13}}+\frac{\gamma_2^4n^8\beta^8}{g_{31}}\Big]\Big\rangle w_m^4+\cdots\Big\} \tag{2.14}$$

$$\delta_x=\lambda_s\gamma_2+\frac{1}{32}\frac{m^2}{\beta^2}(1+2\mu_1)w_m^2+\frac{1}{256}\frac{m^2}{\beta^2}$$
$$\cdot(1+\mu_1)^2(1+2\mu_1)^2\Big[\frac{m^4}{g_{13}}+\frac{\gamma_2^2n^4\beta^4}{g_{31}}\Big]w_m^4+\cdots \tag{2.15}$$

其中

$$\mu_1=A_{11}^{*}\varepsilon/A_{11}^{(1)}\varepsilon \tag{2.16}$$

$$A_{11}^{(1)}\varepsilon=w_m+\frac{1}{16}(1+\mu_1)^2(1+2\mu_1)\Big[\frac{m^4}{g_{13}}+\frac{\gamma_2^2n^4\beta^4}{g_{31}}\Big]w_m^3+\cdots \tag{2.17}$$

及

$$\left.\begin{aligned}g_{13}&=(m^4+18\gamma_1m^2n^2\beta^2+81\gamma_2^2n^4\beta^4)(1+\mu_1)\\&\quad-(m^4+2\gamma_1m^2n^2\beta^2+\gamma_2^2n^4\beta^4)\\g_{31}&=(81m^4+18\gamma_1m^2n^2\beta^2+\gamma_2^2n^4\beta^4)(1+\mu_1)\\&\quad-9(m^4+2\gamma_1m^2n^2\beta^2+\gamma_2^2n^4\beta^4)\end{aligned}\right\} \tag{2.18}$$

2.2 卸载曲线

卸载过程为弹性的，因此采用弹性方程，即式(2.7)仍然有效。此时假定方程(2.1)、(2.2)的解为如下渐近展开式

$$w(x,y,\varepsilon)=\sum_{k=1}\varepsilon^k w_k(x,y),\ \varphi(x,y,\varepsilon)=\varphi_0-\sum_{k=1}\varepsilon^k\varphi_k(x,y) \tag{2.19}$$

无量纲初挠度重新写成如下形式

$$w^*(x,y,\varepsilon)=\varepsilon A_{11}^{*}\sin mx\sin ny=\varepsilon^4\mu_1 A_{11}^{(4)}\sin mx\sin ny \tag{2.20}$$

将式(2.19)、(2.20)代入方程(2.1)、(2.2)，同样可以得到各级摄动方程，采用文[3]类似的摄动步骤，我们可以得到如下大挠度渐近解

$$w=\varepsilon^4[A_{11}^{(4)}\sin mx\sin ny]+\varepsilon^6[A_{13}^{(6)}\sin mx\sin 3ny+A_{31}^{(6)}\sin 3mx\sin ny]+O(\varepsilon^8) \tag{2.21}$$

$$\varphi=\varphi_0-\varepsilon^2\Big[-B_{00}^{(2)}\frac{y^2}{2}+B_{20}^{(2)}\cos 2mx+B_{02}^{(2)}\cos 2ny\Big]$$
$$-\varepsilon^4[-B_{00}^{(4)}y^2/2]-\varepsilon^6[-B_{00}^{(6)}y^2/2]+O(\varepsilon^8) \tag{2.22}$$

其中

$$\left.\begin{aligned}
&\beta^2B_{00}^{(2)}=\frac{1}{8}\frac{m^4+n^4\beta^4}{m^2}A_{11}^{(1)}A_{11}^{(1)}\\
&\beta^2B_{00}^{(4)}=\frac{1}{64m^2}\Big[\frac{m^8}{g_{13}}+\frac{n^8\beta^8}{g_{31}}\Big](1+\mu_2)A_{11}^{(1)}A_{11}^{(1)}A_{11}^{(1)}A_{11}^{(1)}\\
&\beta^2B_{00}^{(6)}=-\frac{1}{512m^2}\Big[\frac{m^8}{g_{13}}\frac{(m^4-8n^4\beta^4)}{g_{13}}+\frac{9n^8\beta^8}{g_{31}}\frac{n^4\beta^4}{g_{31}}\Big]\\
&\qquad\cdot(1+\mu_2)^2A_{11}^{(1)}A_{11}^{(1)}A_{11}^{(1)}A_{11}^{(1)}A_{11}^{(1)}A_{11}^{(1)}
\end{aligned}\right\} \tag{2.23}$$

其它系数同样皆可表为$A_{11}^{(1)}$的形式，如

$$\left.\begin{aligned}
&A_{11}^{(4)}=\frac{1}{8}A_{11}^{(1)}A_{11}^{(1)}A_{11}^{(1)}A_{11}^{(1)}\\
&A_{13}^{(6)}=-\frac{1}{64}\frac{m^4}{g_{13}}(1+\mu_2)A_{11}^{(1)}A_{11}^{(1)}A_{11}^{(1)}A_{11}^{(1)}A_{11}^{(1)}A_{11}^{(1)}\\
&A_{31}^{(6)}=-\frac{1}{64}\frac{n^4\beta^4}{g_{31}}(1+\mu_2)A_{11}^{(1)}A_{11}^{(1)}A_{11}^{(1)}A_{11}^{(1)}A_{11}^{(1)}A_{11}^{(1)}\\
&B_{20}^{(2)}=\frac{1}{16}\frac{n^2\beta^2}{m^2}A_{11}^{(1)}A_{11}^{(1)},\quad B_{20}^{(2)}=\frac{1}{16}\frac{m^2}{n^2\beta^2}A_{11}^{(1)}A_{11}^{(1)}
\end{aligned}\right\} \tag{2.24}$$

其中

$$\left.\begin{aligned}
&g_{13}=(m^2+9n^2\beta^2)^2(1+\mu_2)-(m^2+n^2\beta^2)^2\\
&g_{31}=(9m^2+n^2\beta^2)^2(1+\mu_2)-9(m^2+n^2\beta^2)^2
\end{aligned}\right\} \tag{2.25}$$

进而，我们可以同样导得以最大无量纲挠度为摄动参数的表达式

$$\lambda_x=\lambda_{cr}-\frac{1}{4\sqrt{8}}\frac{m^4+n^4\beta^4}{m^2\beta^2}w_m^{\frac{1}{2}}+\frac{1}{64m^2\beta^2}\Big[\Big(\frac{m^4(m^4+n^4\beta^4)}{g_{13}}$$
$$+\frac{n^4\beta^4(m^4+n^4\beta^4)}{g_{31}}\Big)(1+\mu_2)-2\Big(\frac{m^8}{g_{13}}+\frac{n^8\beta^8}{g_{31}}\Big)\Big](1+\mu_2)w_m$$
$$+\frac{1}{32\sqrt{8}\,m^2\beta^2}\Big[\Big(\frac{m^8}{g_{13}}+\frac{n^8\beta^8}{g_{31}}\Big)\Big(\frac{m^4}{g_{13}}+\frac{n^4\beta^4}{g_{31}}\Big)(1+\mu_2)$$
$$+\Big(\frac{m^8}{g_{13}}\frac{(m^4-8n^4\beta^4)}{g_{13}}+\frac{9n^8\beta^8}{g_{31}}\frac{n^4\beta^4}{g_{31}}\Big)\Big](1+\mu_2)^2w_m^{\frac{3}{2}}+\cdots \tag{2.26}$$

$$\delta_x=\lambda_x+\frac{1}{32}\frac{m^2}{\beta^2}(1+2\mu_2)w_m^2+\cdots \tag{2.27}$$

其中

$$\mu_2=A_{11}^{*}\varepsilon/A_{11}^{(4)}\varepsilon^4 \tag{2.28}$$

$$A_{11}^{(4)}\varepsilon^4=w_m-\frac{1}{\sqrt{8}}(1+\mu_2)^2\Big[\frac{m^4}{g_{13}}+\frac{n^4\beta^4}{g_{31}}\Big]w_m^{\frac{3}{2}}+\cdots \tag{2.29}$$

在卸载曲线式(2.26)中，取

$$\lambda_{cr}=\begin{cases}1 & (对\sigma_{cr}<\sigma_0)\\ \sigma_{cr}b^2t/4\pi^2D & (对\sigma_0\leqslant\sigma_{cr})\end{cases} \tag{2.30}$$

由式(2.14)、(2.26)构成完整的后屈曲平衡路经。

三、结果和讨论

根据渐近分析导出的公式，我们分别按塑性流动理论和形变理论计算了硬铝合金矩形板的后屈曲载荷-挠度曲线（其中宽厚比$b/t=30.0$，$\lambda_0=\sigma_x/\sigma_0$），以及板的缺陷敏感度曲线(其中分别取$b/t=20.0$，30.0和35.0，$\lambda^*=\sigma_{cr}/\sigma_{perf.}$)．材料应力-应变关系如文[14]（表8.1）所给．计算结果如图2，图3所示．现讨论如下

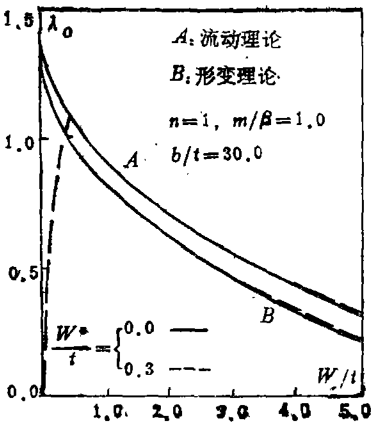

图 2 全过程载荷-挠度曲线

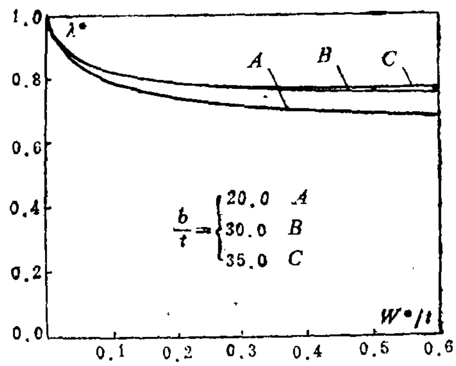

图 3 板非弹性屈曲缺陷敏感度比较

（1） 当有初挠度存在时，弹塑性加载路径和卸载路径构成完整的后屈曲载荷-挠度曲线．可由加载曲线和卸载曲线的交点来确定板的极值点载荷．此时板对初始缺陷表现敏感．

（2） 分别按两种理论计算，板对初始缺陷的敏感程度几乎相同，且随着b/t的增大这种敏感度逐弱．

（3） 根据文[1]的分析，对宽厚比$b/t=30.0$，20.0的板，当初始缺陷$W^*/t=0.1$时，屈曲载荷将下降40～60%．此种缺陷敏感度超过轴压圆柱薄壳弹性屈曲时的情况，令人难以置信．而按本文的分析，屈曲载荷大约下降20%左右．

（4） 初始缺陷对卸载曲线只有微小的影响．

因此，经典塑性流动理论计算结果和实验数据之间的差异可用初始挠度的影响和非弹性屈曲板后屈曲平衡不稳定来解释．

图4为本文计算结果和文[15]实验结果的比较．板的长宽比$\beta=3.0$．图示表明，大部分实验数据落在加载曲线与卸载曲线之间，当计及初挠度$W^*/t=0.3$时，实验结果对整个载荷-挠度曲线有合理的符合．

当宽厚比$b/t=31.8$时(图4a)，$\sigma_{cr}>\sigma_0$，卸载曲线从屈曲点开始．此时，加载曲线与卸载曲线的交点随板初挠度的增加逐趋减值．板对初始缺陷表现敏感．

当宽厚比$b/t=60.8$时(图4b)，$\sigma_{cr}<\sigma_0$，卸载曲线从屈服点开始．此时，加载曲线与卸

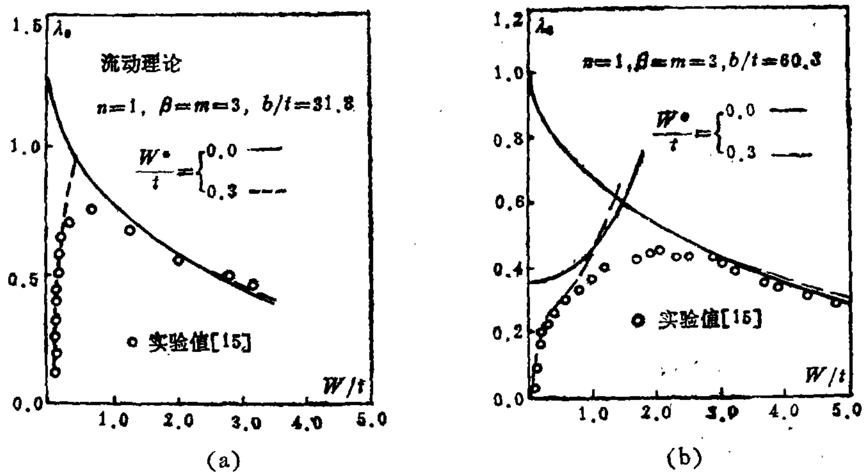

图4 全过程载荷-挠度曲线，理论与实验结果比较

载曲线的交点反随板初挠度的增加逐趋增值。

因此，当计及卸载曲线时，板的非弹性屈曲和弹性屈曲具有完全不同的后屈曲性态。

图 5 为载荷-缩短理论曲线和文［16］实验结果的比较。板的长宽比 $\beta=4.0$，宽厚比 $b/t=79.5$。当计及初挠度 $W^*/t=0.1$时，理论曲线和实验结果有相当好的符合。

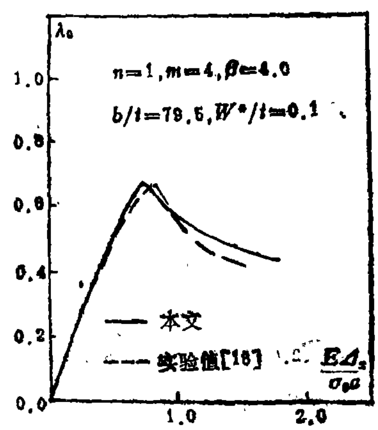

图5 载荷-缩短曲线，理论与实验结果比较

参 考 文 献

［1］ Neale, K. W., Effect of imperfections on the plastic buckling of rectangular plates, *J. Appl. Mech.*, **42** (1975), 115—120.

［2］ Needleman, A., An analysis of the imperfection sensitivity of square elastic-plastic plates under axial compression, *Int. J. Solids Structures*, **12** (1976), 185—201.

［3］ 沈惠申、张建武，单向压缩简支矩形板后屈曲振动分析，应用数学和力学，9，8 (1988)，741—752.

［4］ 沈惠申，正交异性矩形板后屈曲振动分析，应用数学和力学，10，4 (1989)，369—370.

［5］ Rectliffe, A. T., The strength of plates in compression, Cantab Ph. D. Thesis (1968).

［6］ Moxham, K. E., Compression in welded web plates, Ph. D. Thesis, University of Cambridge (1970).

［7］ Frieze, P. A., Ultimate load behaviour of steel box-girder bridges and their components, Ph. D. Thesis, University of London (1975).

[8] Crisfield, M. A., Full-range analysis of steel plates and stiffened plating under uniaxial compression, *Proc. Instn. Civ. Engrs.*, Part 2, **59** (1975), 595—624.

[9] Harding, J. E., R. E. Hobbs and B. G. Neal, The elasto-plastic analysis of imperfect square plates under in-plane loading, *Proc. Instn. Civ. Engrs.*, Part 2, **63** (1977), 137—158.

[10] Little, G. H., The collapse of rectangular steel plates under uniaxial compression, *Structural Engr.*, **58B** (1980), 45—61.

[11] Gradzhi, R. and K. Kowal-Michalska, Collapse behaviour of plates, *Thin-Walled Structures*, **6** (1988), 1—17.

[12] Korol, R. M. and A. N. Sherbourne, Strength predictions of plates in uniaxial compression, *Proc. ASCE*, **98**, ST9 (1972), 1965—1986.

[13] Davies, P., K. O. Kemp and A. C. Walker, An analysis of the failure mechanism of an axially loaded simply supported steel plate, *Proc. Instn. Civ. Engrs.*, Part 2, **59** (1975), 645—658.

[14] Вольмир A. C., *Устойчивость Упругих Систем*, Москва (1963).

[15] Sherbourne, A. N. and R. M. Korol, Postbuckling of axially compressed plates, *Proc. ASCE*, **98**, ST10 (1972), 2223—2234.

[16] Moxham, K. E., Buckling tests on individual welded steel plates in compression, Cambridge University Report No. CUED/C-Struct/TR3 (1971).

[17] Dawe, J. L. and G. Y. Grondin, Inelastic buckling of steel plates, *Proc. ASCE*, **111**, ST1 (1985), 95—107.

[18] Bradfield, C. D. and W. P. Stonor, Simple collapse analysis of plates in compression, *Proc. ASCE*, **110**, ST12 (1984), 2976—2993.

Elasto-Plastic Analysis for the Buckling and Postbuckling of Rectangular Plates under Uniaxial Compression

Shen Hui-shen

(*Shanghai Jiaotong University, Shanghai*)

Abstract

Full-range analysis for the buckling and postbuckling of rectangular plates under in-plane compression has been made by perturbation technique which takes deflection as its perturbation parameter.

In this paper the effects of initial geometric imperfection on the postbuckling behavior of plates have been discussed. It is seen that the effect of initial imperfection on the inelastic postbuckling of plates is sensitive. By comparison, it is found that the theoretical results of this paper are in good agreement with experiments.

Key words structural stability, inelastic buckling, postbuckling rectangular plate